MULTIDISCIPLINARY SCIENCE JOURNAL

TYPE OF THE PAPER
Published Online: August 24, 2023
https://doi.org/10.31893/multiscience.2024027

Simulation study of mobile phone radiation thermal effect in human heart tissue

Khitam Elwasife[a] | **Eqbal Radwan**[b] | **Ghadir Yasin**[a]

[a]Department of Physics, Faculty of Science, Islamic University of Gaza, Palestine.
[b]Department of Biology, Faculty of Science, Islamic University of Gaza, Palestine.

Abstract The public's concern over potential health risks related to the absorption of electromagnetic radiation (EMR) has been developing due to the prolonged use of cell phones close to the human body, particularly the human heart. To address these issues, this study aims to present a numerical simulation of EMR in the spectral range (900 MHz, 1800 MHz, and 2400 MHz) on human heart tissue using a Matlab program and the Finite-Difference Time-Domain (FDTD) method in One Dimension (1D). A mathematical analysis of electromagnetic radiation heating equations in a one-dimensional, one-layer model has also been discussed by numerically calculating the transient bioheat transfer equation and Maxwell's equations by using the FDTD to predict the effects of thermal physics properties on the transient temperature of human heart tissue. The results revealed that FDTD is an efficient method to evaluate the thermal effect of EMR due to its perfect boundary condition. It was found that the heart tissue reacts more at 900 MHz compared to 1800 MHz and 2400 MHz, and the tissue absorption is higher at the lower frequency. The effects of various parameters on the temperature increase in the human heart tissue were considered, such as the electric field, magnetic field, thicknesses, and thermal conductivity of the heart tissue. It was found that the frequency most affecting the tissue was 900 MHz. Our study found that the temperature distribution decreases with an increase in tissue thickness. We note that the results are similar for the different frequencies. It turns out that as the thermal conductivity of the heart tissue increases, the temperature distribution decreases slightly, while no change occurs here in the relationship between thermal conductivity and the temperature distribution of tissue with the change in the frequency of a wave.

Keywords: Electromagnetic radiation, transient bioheat transfer equation, heart rate, Maxwell's equations, FDTD method

1. Introduction

Our daily lives have been significantly impacted by the rapid technological advancements in electronics, electro-optics, and computer science. The biological consequences of electromagnetic (EM) radiation have also given rise to safety concerns, particularly with long-period exposure. In recent years, people have been using mobile phones and other cellular devices more frequently than at any other time due to their advantages and importance in our daily lives. Long-term use will expose the user to high-frequency EMR, which has been linked to serious diseases like brain cancer and Alzheimer's. The community's concern over rising radiation exposure has led to an increase in research into how emissions may affect human health. The kinetic energy of charged particles is transferred from the applied electric field to the human body parts, particularly the head and heart, during the device's operation (Ismail 2007). It is necessary to take into account a range of waves and signals, including digital signals found in systems for digital radio, digital television, and digital mobile phones, as well as pure or nearly pure sine waves. The field has advanced considerably, necessitating a high level of competence to set safety guidelines or standards and take appropriate measurements (Vander Vorst et al 2006; Romanenko et al 2017; Haemmerich et al 2022).

In many medical applications, such as thermal therapeutic treatments that depend on knowledge of temperature variations occurring in the body, the study of transport phenomena, particularly heat transmission within the human body, is of utmost relevance. Evaluation of the thermal effects of EMR exposure becomes essential. The threshold limit of safe exposure needs to be established due to the rising use of high-power EM waves (Goyal and Vafai 2017). The peak spatial average specific absorption rate (SAR) is the basis for laws governing how much electromagnetic field exposure is safe for humans. The temperature of tissues rises as a result of power absorption. The proper operation of biological organs may be adversely affected by this temperature increase. A slight rise in body temperature (1–5°C) can impair a number of bodily functions, including short-term infertility, changes in hormone synthesis and blood chemistry, and inhibition of the immune system (Hirata et al 2013; Morimoto et al 2016; Seetharaman et al 2022). When evaluating potential health risks, SAR values

 Received: June 11, 2023 | Accepted: August 8, 2023

are crucial, and to make sure the EMR sources are safe to use, these values are compared to a safety limit established by the International Commission on Non-Ionizing Radiation Protection (ICNIRP) (Aerts et al 2023; Yi et al 2023).

The impacts of thermal physics characteristics on the transmission temperature of biological tissue were predicted by numerically calculating the transient bioheat transfer equation and Maxwell's equations by using the finite difference method (Elwasife et al 2023). This prognosis of the temperature increase in biological bodies can be employed in medical procedures as a useful tool for thermal diagnostics. Many physiologists, physicians, and engineers have expressed an interest in mathematical modeling of the complicated thermal interaction between vasculature and tissue. Harry H. Pennes, a researcher at Columbia University's College of Physicians and Surgeons, produced the first quantitative relation characterizing heat transfer in human tissue on a continuous basis, which included the effects of blood inflow on tissue heat (Charny 1992). Dissecting the complex physicochemical environment of the staining system, we developed a highly optimized 3D staining imaging pipeline based on CUBIC. Based on our precise characterization of biological tissues as electrolyte gels (Susaki et al 2020), A mathematical model formulated for 3D coupled blood flow, heat transfer, and resistive heating in the cardiac chamber during the RFCA process for arrhythmia has been evaluated (Wongchadakul et al 2023).

Temperature fields surround all biological bodies that are dependent on their surroundings; that is, organs and tissues do not have consistent temperatures. Even inside a single organism, the temperature fields' non-uniformity causes energy transfer between tissues via perfused blood (Xu et al 2009). Many variables influence the heat of the body of a human, including environmental conditions, the medium temperature surrounding tissues, muscle metabolism, and blood circulation (Hristov et al 2019). In biological tissues, voids separate dispersed cells. Blood enters those tissues through veins and arteries and travels through blood capillaries to the tissue cells. Capillary blood returns to the heart via veins, where it accumulates before being pushed back to the heart. Thermic conductivity, blood perfusion, and heat obstetrics all contribute to energy transmission in tissues. Some works review the relevant literature with a focus on transport processes, especially the potential role of diffusion and advective flows (Ray and Heys 2019).

In the study of Wessapan and Rattanadecho (2012), they performed a numerical analysis of the SAR and heat transfer that take place in the human body when exposed to various EMR frequencies. Also, Keangin et al (2013) conducted a numerical analysis of the treatment of liver cancer. Many scientists have investigated how heat moves through biological material while taking into account perfusion, thermal conduction within tissues, convective blood flow, and heat production during metabolism. Blood flows through multiple blood vessels in a biological tissue, which can be thought of as a microvascular bed (Khaled and Vafai 2003).

Heat transmission in lively tissues is a complex process, and arithmetical modeling must be simplified to allow the use of its methods. The properties of the ECM have been thoroughly used in tissue engineering and regenerative medicine research, aiming to restore the function of damaged or dysfunctional tissues. It is shown that applications of ECM-derived components are multiple, from in vitro stem cell basic research to clinical settings (Mendibil et al 2020). Heat transfer procedures in medical implementations, such as cryosurgery, laser thermal, radio-frequency, and thermic resections, ablations, ultrasound, and so on, necessitate not just empirical data but also a thorough understanding of fundamental heat transport mechanisms and appropriate mathematical modeling (Yamazaki et al 2006). Some reviews explained the master techniques to have blood flow, the factors that alter blood flow in the skin, and how aging and diabetes affect blood flow. Recommendations for the measurement of resting blood flow are presented (Petrofsky 2012).

For almost a century, scientists have examined the impact of blood flow on heat transmission in living tissue, beginning with Bernard's experiments in 1876 (Charny 1992). The bioheat equation proposed by Pennes, which is regarded as one of the models for energy transfer in tissues, is often used to express energy transport in a biological system. The bioheat equation developed by Pennes is the most extensively used thermal model for understanding heat transport in biological systems subjected to electromagnetic waves (Wang et al 2020).

The "Fick principle," as Pennes named it, governs the transport of heat from the blood to the tissue. The rate of mass transfer between blood and tissue, according to this idea, is equal to the difference between a substance's blood and tissue levels multiplied by the rate of blood flow. Pennes thought the total amount of heat imparted from the blood to the tissues Q_p matches with a temperature differential between arterial blood entering the tissue and venous blood exiting the tissue when using this concept to explain the average heat transport among blood and tissues (Charny 1992).

$$Q_p = \omega_b \, \rho_b c_b (T_a - T_v) \qquad (1)$$

Where:

ω_b : blood perfusion rate as a volumetric rate per unit volume of tissue.

ρ_b : the blood density.

c_b : the blood's specific heat.

T_a : the blood that enters the tissue via the arteries.

T_v : the flow of venous blood out of the tissue.

Because the temperature of venous blood is affected by the degree of thermal equilibration it experiences with the surrounding tissue, Pennes developed the k' thermal equilibration parameter to calculate this impact.

$$T_v = T_t + k'(T_a - T_t) \qquad (2)$$

when $k' = 0$, i.e., complete thermal equilibration, that's mean the venous blood temperature leaving the tissue is $T_v = T_t$, while if $k' = 1$, the venous blood leaves the tissues at temperature same to temperature of blood inside the arteries$T_v = T_a$.

T_a is constant anywhere the tissue in the Pennes derivation at times T_b, and k' is close to zero everywhere, i.e. $T_v = T_t$, as a result, the familiar The phrase "Pennes perfusion heat source" refers to a heat source that is perfused.

$$Q_p = \omega_b \rho_b c_b (T_b - T_t) \qquad (3)$$

Where:

T_b : is the blood temperature
T_t : is the tissue temperature

The perfusion heat source in Equation (3) assumes that blood enters the smallest vessels of the microcirculation (blood flow through the smallest vessels in the circulatory system, such as arterioles, venules, shunts, and capillaries) at temperature T b, where all heat transfer between blood and tissue occurs. When blood exits the capillary, it has completed thermal equilibration with the surrounding tissue and enters the venous circulation at this temperature; the venous blood temperature is expected to remain at the tissue temperature. There is no heat exchange in this area of the microcirculation. As a result, the Pennes perfusion phrase ignores all precapillary and postcapillary heat exchange between blood and tissue. All heat exchange between blood and tissue occurs in the bigger channels of the microcirculation before arterial feed blood reaches the capillaries, and similarly, some heat exchange with the surrounding tissue might occur after blood exits the capillary. By ignoring axial gradients in tissue temperature and assuming angular symmetry, The Pennes equation is:

$$\rho c_p \frac{\partial T_t}{\partial t} = k \frac{\partial^2 T_t}{\partial x^2} + \omega_b \rho_b c_b (T_b - T_t) + Q_m \qquad (4)$$

Whereas:

ρ : tissue's density
c_p : tissue's specific heat
k : tissue's thermal conductivity.
Q_m : the steady rate of metabolic heat obstetrics in tissue's layers

Penne's equation has been used in a variety of biological research studies and has been shown to be highly useful. A simulation technique and Pennes equation were used to evaluate the steady-state temperature distribution within the brain after a head injury (Zhu and Diao 2001). Deng and Liu used the Pennes equation to analyze the influence of pulsatile blood perfusion on tissue temperature (Liu and Ockerman 2001). Thermal characteristics and geometrical dimensions have been studied in relation to skin burn injuries (Bai et al 2002).

On the other hand, Chua et al (2002) offered a differentiation of 1- and 2-dimensional systems for predicting the condition of skin burns. The impact of microwave heating on biological tissue thermodynamic conditions has even been investigated (El-Dabe et al 2003). Weinbaum and Jiji (1985) relied on the theory that Because the small arteries and veins are parallel and the influx direction is countercurrent, the heating and cooling effects are balanced. The isotropic blood perfusion term in the Pennes equation is negligible as a result of this type of tissue vascularization. It also makes the tissue act as an anisotropic heat transfer medium. As a result, by changing the diameters and orientations of the vessels, Weinbaum and Jiji (1985) replaced the thermic conductivity in the Pennes equation with a conductivity that is effective and is proportional to the blood perfusion rate. They also discovered that in locations where the countercurrent vessels are less than 65–70 ml in diameter, isotropic blood perfusion between them can have a major effect on heat transmission (Zhu et al 2019).

There is a deep scarcity of previous studies regarding the coupling of EMR with heat transfer based on the Finite-Difference Time-Domain (FDTD) method. The coupled equations were solved by Keangin et al (2013) using the finite element method (FEM), which produced temperature profiles for blood and tissue at various electromagnetic wave powers and electromagnetic wave frequencies. In their investigation, they took into account six different biological mediums. It is more effective to employ an analytical solution when a lot of parameters are required for the study. Surface heating for planar geometry is the focus of the literature that is currently available on analytical solutions. For the Pennes bioheat transfer equation, Liu (2001) carried out the uncertainty analysis and came up with an analytical solution.

Overall, blood vessels, cells, and interstitial space can be considered the main three constituents of biological tissue medium. The biological medium is further divided into extravascular and vascular regions (blood vessels). In this study, the extravascular region is regarded as the tissue (solid matrix) phase, whereas the vascular portion is designated the blood phase (Figure 1). The anatomical structure is represented as a blood-saturated tissue in this study's model, which is a porous medium matrix through which blood escapes. The electromagnetic field emitted by high-power radiation sources can be detrimental to human health. High-intensity electromagnetic radiation is widely known for its ability to seriously thermally harm the body's fragile tissues (Goyal and Bhargava 2018).

To investigate hotspot zones inside the body, it is therefore vital to investigate temperature distribution profiles and how they vary as a result of electromagnetic waves. Since it is obviously impossible to subject a living human being to electromagnetic fields during an experiment, an attempt has been made to create a realistic model that can be replicated using numerical methods. This study takes into account a homogenous, thermally completely formed, and isotropic two-dimensional body. It is assumed that the blood flow is constant and incompressible. Inside the biological medium, no chemical reactions or phase transitions take place. The thermodynamical characteristics of both blood and solid matrix (tissue) are taken into account to be inconsequential, and natural convection is insignificant enough to be disregarded (Shbanah and Kovács 2022).

The current study offers a thorough analytical solution for investigating the effect of EMR on cardiac tissue. Therefore, this study aims to present a numerical simulation of EMR in the spectral range (900 MHz, 1800 MHz, and 2400 MHz) on the human heart tissue by Matlab and the Finite-Difference Time-Domain (FDTD) method in One Dimension (1D). We believe that this is a unique analytical explanation of the impact of electromagnetic fields on biological materials like the human heart. Due to the analytical solution's excellent agreement with the results of the full numerical simulation and the experiments, as well as the fact that it offers a quick way for examining and simulating diverse electromagnetic field effects on biological materials, this fact alone makes the work unique and extremely significant.

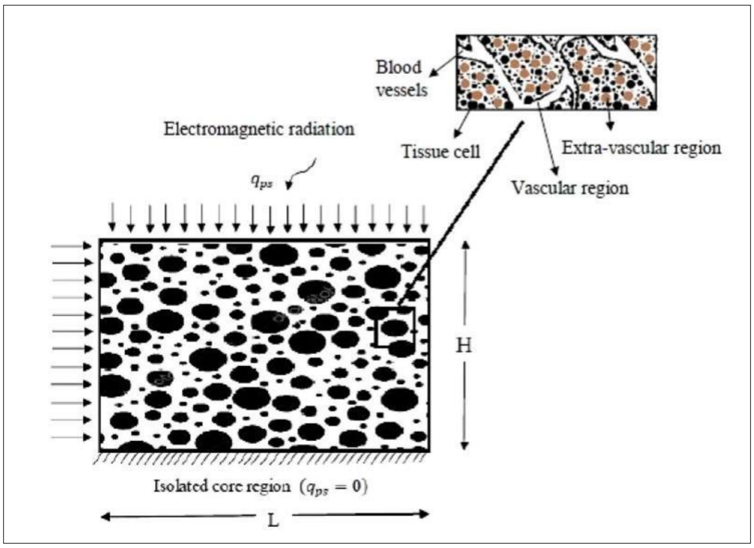

Figure 1 Schematic of exposure of a living organ to EMR (Goyal and Vafai 2017).

2. Mathematical formulation

2.1. Theory and model

The graph of 1-layer tissue model in 1-dimensional is indicated in the next chart (Figure 2).

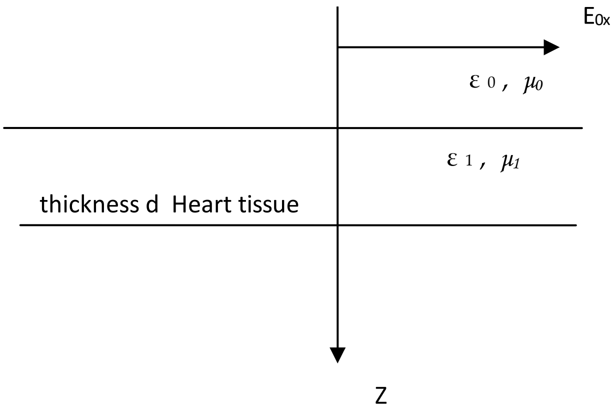

Figure 2 The outline of 1-dimensional,1-layer heart tissue thickness (d) model.

The temperature, electric field and magnetic field supposed respectively by $T = T(z,t)$, $E = (E(z,t), 0,0)$, $H = (0, H(z,t), 0)$. Because the square of the modulus of the E-field intensity is connected to the heat sources emanating from electromagnetic radiation, Max's Eq. along with the bioheat Equation. may be stated as:

$$\frac{\partial H}{\partial z} + \frac{\partial E}{\partial t} + \sigma E = 0 \qquad (5)$$

$$\frac{\partial E}{\partial z} + \mu \frac{\partial H}{\partial t} = 0 \qquad (6)$$

$$\rho c_p \frac{\partial T_t}{\partial t} = \frac{\partial}{\partial z}\left(k \frac{\partial T_t}{\partial z}\right) + \omega_b \rho_b c_b (T_b - T_t) + Q_m (T_t)|E|^2 \qquad (7)$$

The analysis supposes that there is no resistance between two surfaces, the sources of heat and the heart. As a result, the surface temperature remains consistent during the exposure. Within the layer, the tissue is assumed to be homogenous. Thermic conductivity and heat capacity are regarded as constants. The term on the left of Equation (7) is created by a temperature gradient, represents energy storage in tissue the 2nd idiom shows heat transmit between tissue and microcirculatory blood perfusion, and the term E2 is the E-power density preserved in tissue. For the solution of partial differential equations, the next limits and starting conditions were desired.

$$T(z,0) = \frac{T_C Z}{L} \qquad T(L,t) = T_C \qquad T(0,t) = 0 \qquad (8)$$

$$E(z,0) = \frac{E_0 Z}{L} \qquad E(L,t) = E_0 \qquad E(0,t) = 0 \qquad (9)$$

$$H(z,0) = \frac{H_0 Z}{L} \qquad H(L,t) = H_0 \qquad H(0,t) = 0 \qquad (10)$$

We can presume that the body heating point is of the next shape:
$Q(T) = T^m$. consider the following non-dimensional variable:

$$\lambda = \frac{L^2 T_b^{m-1} |E_0^2|}{v \rho c_p} \qquad (11)$$

$$\lambda_1 = \frac{v \varepsilon E_0}{L H_0} \qquad (12)$$

$$\lambda_2 = \frac{L \sigma E_0}{H_0} \qquad (13)$$

$$\lambda_3 = \frac{v \mu H_0}{L E_0} \qquad (14)$$

$$\rho_1 = \frac{\rho_b}{\rho} \qquad c_1 = \frac{c_b}{c_p} \qquad \omega_1 = \frac{\omega_b L^2}{v} \qquad (15)$$

The dimensional Maxwell's, & equations of energy can be formed as:

$$\frac{\partial H}{\partial z} + \lambda_1 \frac{\partial E}{\partial t} + \lambda_2 E = 0 \qquad (16)$$

$$\frac{\partial E}{\partial z} + \lambda_3 \frac{\partial H}{\partial t} = 0 \qquad (17)$$

$$\frac{\partial T}{\partial t} = \frac{1}{\rho}\frac{\partial^2 T}{\partial z^2} + \omega_1 \rho_1 c_1 (1 - T) + \lambda |E|^2 T^m \qquad (18)$$

We suppose the E-field dampen increasingly with displacement.

$$|E|^2 = E_0^2 e^{-kx} \qquad (19)$$

For a specific stable E_0 & and k. We resolve Maxwell's Eq. and numerically solve the bioheat transmit equation, and make the assumption m=1.

2.2. Numerical technique

To solve Maxwell's Eq. as well as the bioheat transient Equation, that explains the heart sear process induced by high-heat supplies being applied to heart tissue, a one-dimensional finite difference time domain approach is utilized. Because the spatial and time steps are small and adequate to make certain The transient temperature is mesh independent, the group of partial equation that differ. was solved using the finite difference technique, yielding the difference Equation below:

$$\frac{\partial E}{\partial t} = -\frac{1}{\lambda_1}\frac{\partial H}{\partial z} - \frac{\lambda_2}{\lambda_1}E \quad (20)$$

$$\frac{E_x^{n+1/2}(k) - E_x^{n-1/2}(k)}{\Delta t} = -\frac{1}{\lambda_1}\left[\frac{H_y^n(k+1/2) - H_y^n(k-1/2)}{\Delta z}\right] - \frac{\lambda_2}{\lambda_1}\left[\frac{E_x^{n+1/2}(k) + E_x^{n-1/2}(k)}{2}\right] \quad (21)$$

$$E_x^{n+1/2}(k) = \frac{\left(1 - \frac{\lambda_2 \Delta t}{2\lambda_1}\right)}{\left(1 + \frac{\lambda_2 \Delta t}{2\lambda_1}\right)} E_x^{n-1/2}(k) - \frac{\left(\frac{\Delta t}{\Delta z.\lambda_1}\right)}{\left(1 + \frac{\lambda_2 \Delta t}{2\lambda_1}\right)}\left[H_y^n(k+1/2) - H_y^n(k-1/2)\right] \quad (22)$$

Similarly, the magnetic field becomes:

$$H_y^{n+1}(k) = H_y^{n-1/2}(k) + \frac{\Delta t}{\Delta z.\lambda_3}\left[E_x^n(k-1/2) - E_x^n(k+1/2)\right] \quad (23)$$

And the bioheat equation solved as:

$$T^{n+1/2}(k) = \frac{\frac{-\Delta t}{p\Delta z^2}}{1 - \frac{\omega_1\rho_1 c_1}{2} + \frac{\lambda}{8}\left(E_x^{n+1/2}(k) - E_x^{n-1/2}(k)\right)}\left[T^n(k+1/2) - 2T^n(k) + T^n(k-1/2)\right] - \omega_1\rho_1 c_1 + \left(\frac{\omega_1\rho_1 c_1}{2} - \frac{\lambda}{8}\left(E_x^{n+1/2}(k) - E_x^{n-1/2}(k)\right)\right)T^{n-1/2}(k) \quad (24)$$

3. Results and Discussion

A one-dimensional layer transient finite-difference model for expecting temperatures in lively tissues, including tissue from the heart, when exposed to electromagnetic radiation heating is shown. The impacts of numerous variables on the temperature increase in tissue from the human body, such as E-field values, M-field values, tissue thicknesses, and the heat conductivity of the tissue, are studied in the tissue's transmission of heat.

Figures illustrate the effect of three different values of the E-field at 900 MHz in space on the temperature spreading in heart tissue. We used a parameter of human blood such as specific heat that equals 3770, density that equals 1060, and the blood perfusion rate that equals 0.00125 (El-dabe et al 2003; Zhu and Bischof 2019). As for human tissue, we have the value of specific heat equal to 3600 (Giering et al 1995), the density of heart tissue equal to 1030, the thermal conductivity of human tissue equal to 0.2, and the distance to the body core equal to 0.002. The thermal effect of electromagnetic radiation on the eye retina has been studied (Elwasife 2012).

It can be observed that when E0 rises, the temperature distribution increases. We also note that from 0 to 2 in space steps, we have decreased exponentially; from 2 to 4, We have a small increase; from 4 to 6, the temperature changed from 1.3 to 1.7; and then from 6 to 10, we have a high increase. When we changed the frequency to 1800 MHz, we did not get a change in temperature at E0 = 2, and E0 = 3, while at E0 = 4, we found a noticeable increase in temperature. Also, when we changed the frequency to 2400 MHz, we only had a slight change at E0 = 4, which was barely noticeable. Penne's bioheat transfer equation was solved analytically to calculate the long-time exposure effect and temperature rise. The results show that by changing the frequency, the value of temperature does not change; also, from the results and running the program, the curve changes according to the parameter of the electric and magnetic fields.

Figures also show the relation between the magnetic field in the free space H and the temperature distribution. It is seen that the temperature distribution slightly increases as H (the magnetic field) decreases. And we find that from 0 to 2 in space steps, we have a decrease exponential, from 2 to 6, We have a low increase, and from 6 to 10, we have a more significant increase. We also note that the increase in temperature in the space steps from 8 to 10 at H0=2 ranges from 1.4 to 1.44. In the next figure that describes the relationship between the magnetic field in the free space H and the temperature distribution at 1800 MHz, we find that the increase in temperature in the space steps from 8 to 10 at H0 = 2 ranges from 1.4 to 1.41, while at 2400 MHz, the temperature distribution is lower compared to the frequencies of 1800 MHz and 900 MHz (Figures 3–14).

The temperature distribution against space coordinates for different thicknesses of tissue (L = 0.001, 0.002, 0.0002) is shown. We find that the temperature distribution decreases with an increase in tissue thickness. We note that the results are similar for the different frequencies. According to the previous study on another tissue such as dura (Elwasife 2019), when the thickness is 0.002 and the electric field is 4 v/m, we noticed that the temperature is very different. When working on a different tissue than Dura in previous research and comparing the results, we found a large difference in temperature, as the value reached 60 in the case of Dura, while it reached 3 at the same parameter but with different dielectric properties. In the case of the heart tissue, due to its characteristics, we noticed that the tissue is more sensitive. The distribution of electric field in dura tissue is very small compared with other tissues, such as prostate tissue exposed to cellular phone radiation, but in the case of this study, by changing the amplitude of the electric field, the curves are changing. By using variable values of the electric field, we found that the temperature changes significantly, especially when the value of the electric field is low compared to the value of 2 or 3 v/m. Another explanation is that when using variable values of the magnetic field, the increase was rather small, as shown in Figures 6, 7, and 8.

The three previous numbers clarify the effect of the three different thermal conductivity values of human heart tissue on the transition temperature. It turns out that as the thermal conductivity of the heart tissue increases, the temperature distribution decreases slightly, while no change occurs here in the relationship between thermal conductivity and the temperature distribution of tissue with the change in the frequency of a wave.

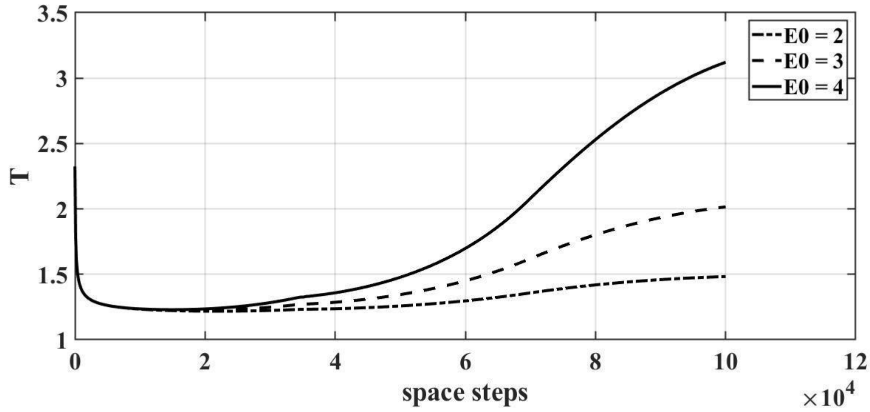

Figure 3 The relation between temperature and space steps with radiation for different electric fields (E0 = 2, 3, 4), where f=900MHZ, cb = 3770, ρb = 1060, ωb =.00125, cp = 3600, ρp = 1030, k = 0.24, L = 0.002, H0 = 1.

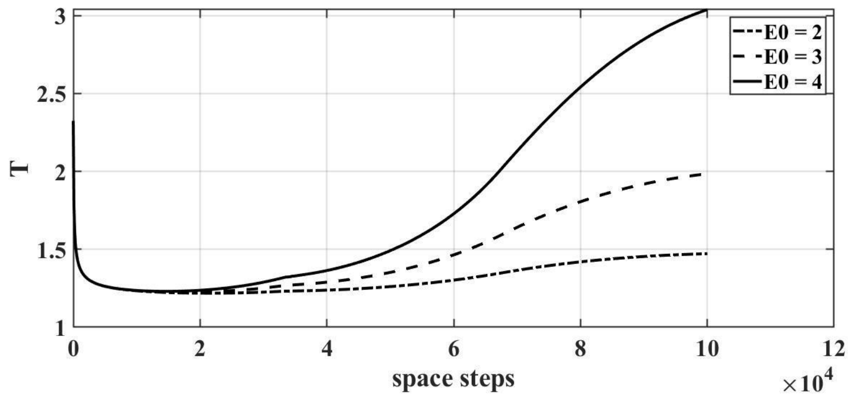

Figure 4 The relation between temperature and space steps with radiation for different electric fields E0 = 2, 3, 4, where f = 1800 MHZ, cb = 3770, ρb = 1060, ωb =.00125, cp = 3600, ρp = 1030, k = 0.24, L = 0.002, H0 = 1.

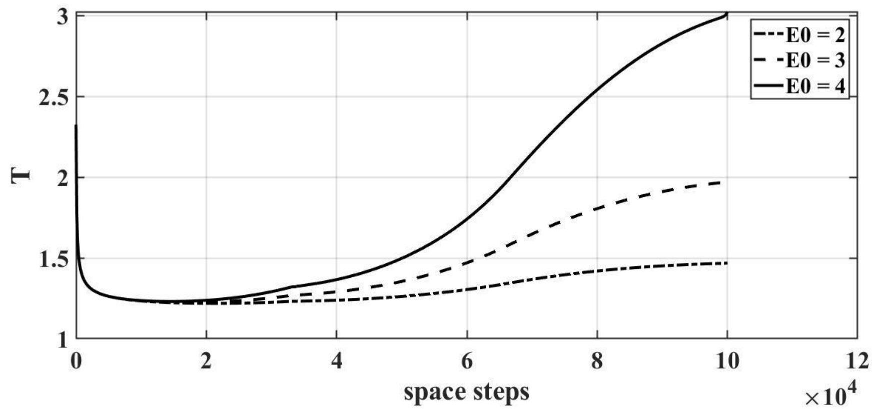

Figure 5 The relation between temperature and space steps with radiation for different electric fields E0 = 2, 3, 4, where f = 2400 MHZ, cb = 3770, ρb = 1060, ωb = 0.00125, cp = 3600, ρp = 1030, k = 0.24, L = 0.002, H0 = 1.

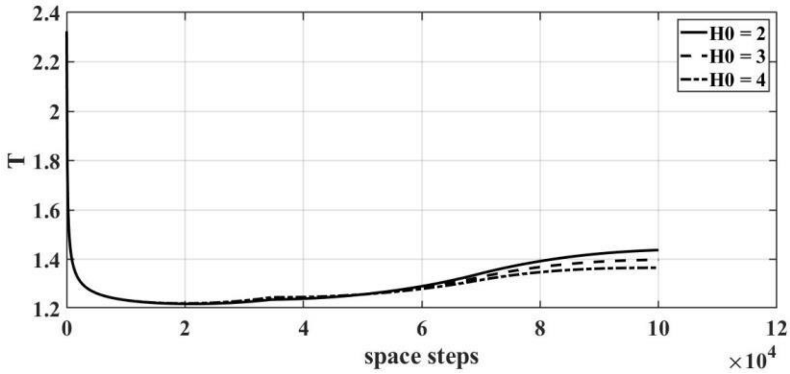

Figure 6 The relation between temperature and space steps with radiation for different values of the magnetic field H0 = 2, 3, and 4, where f = 900 MHZ, cb = 3770, ρb = 1060, ωb = .00125, cp = 3600, ρp = 1030, k = 0.24, L = 0.002, E0 = 2.

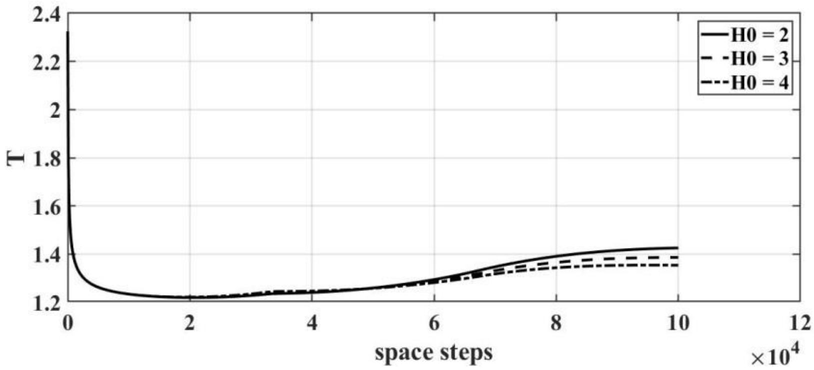

Figure 7 The relation between temperature and space steps with radiation for different values of the magnetic field H0 = 2, 3, and 4, where f = 1800 MHZ, cb = 3770, ρb = 1060, ωb = .00125, cp = 3600, ρp = 1030, k = 0.24, L = 0.002, E0 = 2.

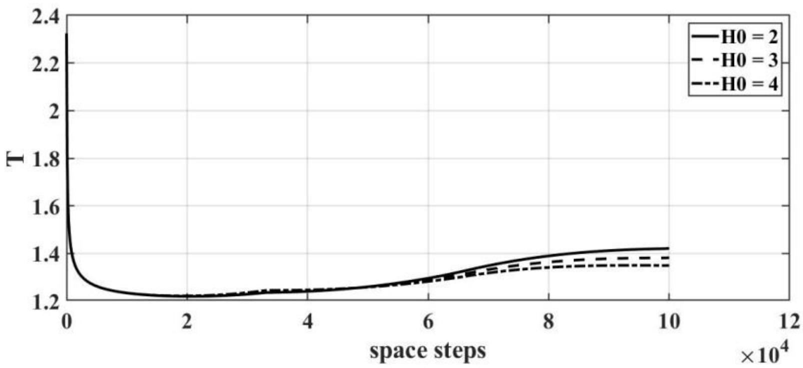

Figure 8 The relation between temperature and space steps with radiation for different values of the magnetic field H0 = 2, 3, and 4, where f = 2400 MHZ, cb = 3770, ρb = 1060, ωb = 0.00125, cp = 3600, ρp = 1030, k = 0.24, L = 0.002, E0 = 2.

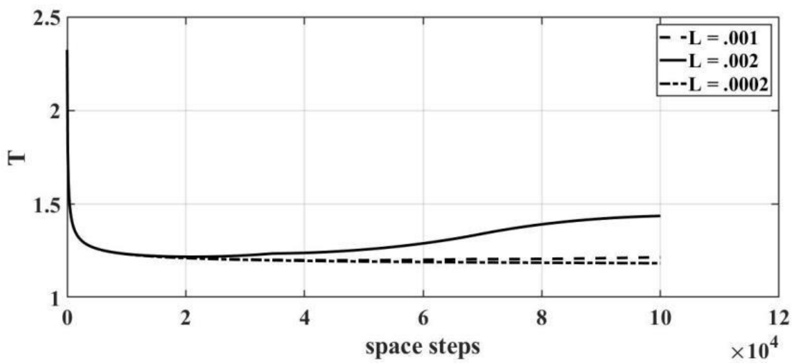

Figure 9 The relation between temperature and space steps with radiation thickness of tissue L = 0.001, 0.002, 0.0002, where f = 900MHZ, cb = 3770, ρb = 1060, ωb = 0.00125, cp = 3600, ρp = 1030, k = 0.24, H0 = 2, E0 = 2.

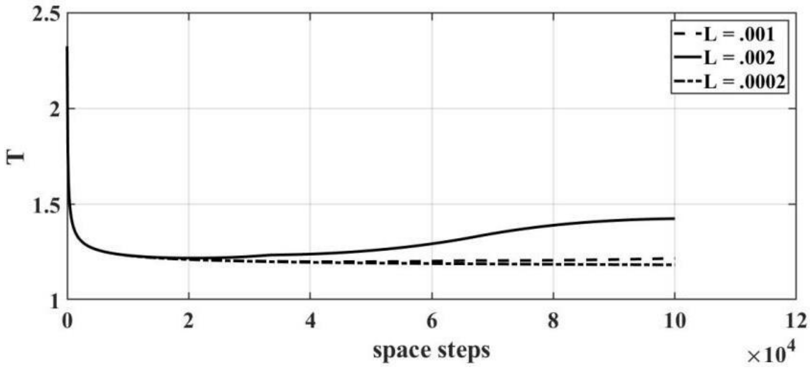

Figure 10 The relation between temperature and space steps with radiation for different thicknesses of tissue L = 0.001, 0.002, 0.0002, where f = 1800 MHZ, cb = 3770, ρb = 1060, ωb = 0.00125, cp = 3600, ρp = 1030, k = 0.24, H0 = 2, E0 = 2.

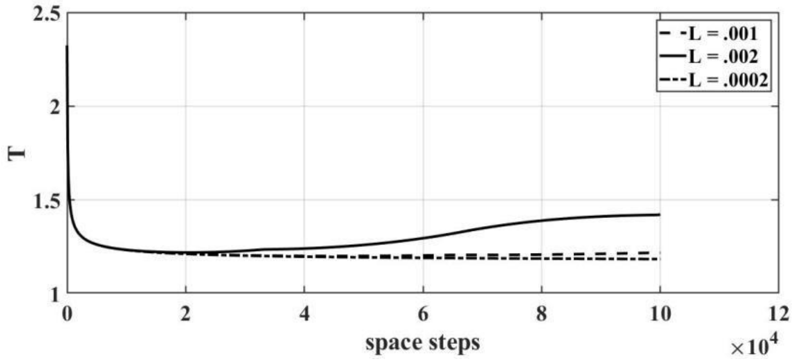

Figure 11 The relation between temperature and space steps with radiation to the thickness of tissue L = 0.001, 0.002, 0.0002, where f = 2400 MHZ, cb = 3770, ρb = 1060, ωb = 0.00125, cp = 3600, ρp = 1030, k = 0.24, H0 = 2, E0 = 2.

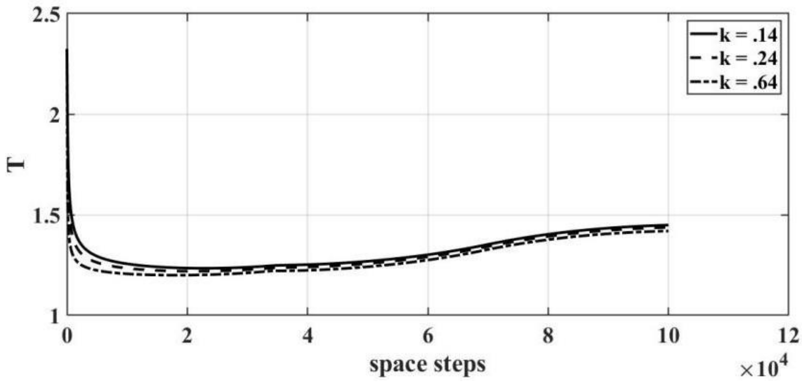

Figure 12 The relation between temperature and time steps with radiation k = 0.14, 0.24, and 0.64, where f = 900 MHZ**,** cb = 3770, ρb = 1060, ωb = 0.00125, cp = 3600, ρp = 1030, L = 0.002 , H0 = 2, E0 = 2.

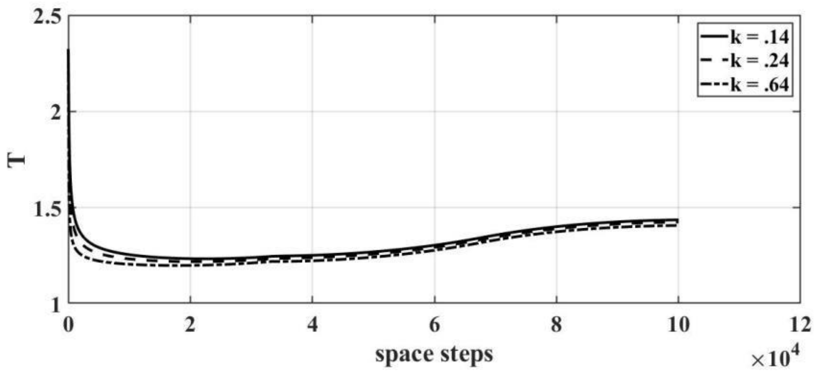

Figure 13 The relation between temperature and time steps with the thermal conductivity of tissue (k = 0.14, 0.24, and 0.64), where f = 1800 MHZ, cb = 3770, ρb = 1060, ωb = 0.00125, cp = 3600, ρp = 1030, L = 0.002 , H0 = 2, E0 = 2.

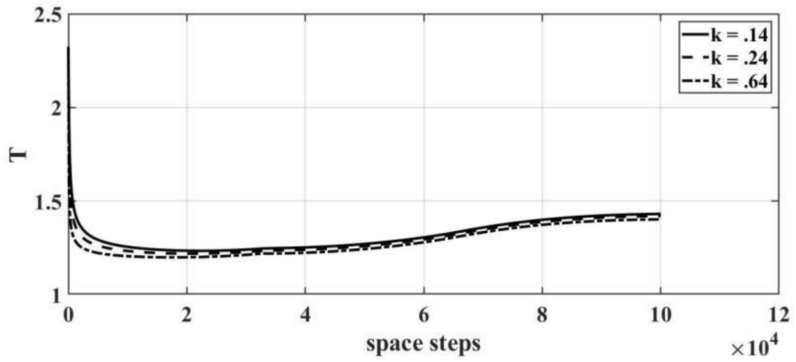

Figure 14 The relation between temperature and time steps with radiation = 2.4 GHZ, where k = 0.14, 0.24, 0.64, and f = 2400 MHZ, cb = 3770, pb = 1060, ωb = 0.00125, cp = 3600, pp = 1030, L = 0.002, H0 = 2, E0 = 2.

4. Conclusions

The current study offers a novel way to calculate the transient bioheat of human heart tissues due to electromagnetic radiation exposure. This study is a numerical simulation of the effect of electromagnetic radiation on human heart tissue, which has been studied using different frequencies. The electromagnetic spectrum (900 MHz, 1800 MHz, and 2400 MHz), the Matlab program, and the Finite-Difference Time-Domain (FDTD) method in one dimension have been used. A new mathematical analysis of electromagnetic radiation heating equations in a one-dimensional, one-layer model has been discussed by numerically calculating the transient bioheat transfer equation and Maxwell's equations by using the finite difference method to predict the effects of thermal physics properties on the transient temperature of human heart tissue. The effects of various parameters on the temperature increase in the human heart tissue were considered, such as the electric field, magnetic field, thicknesses, and thermal conductivity of the heart tissue. It was found that the frequency most affecting the tissue is 900 MHz.

In many diagnostic medical applications, medical devices that emit EMR are used as a thermal therapeutic treatment; therefore, they cause thermal changes in the human body. It is crucial to study transport phenomena, specifically heat transmission through the body. The importance of this study arises from the fact that it is crucial to assess how exposure to EMR affects human heart tissue. Due to the increased use of high-power EMR, the threshold limit of safe exposure needs to be defined.

5. Limitations

The only limitation of this study is that it does not incorporate all commercial cell phone frequencies and the incident power level that humans are exposed to in daily life.

6. Future Work

We suggest studying the numerical simulation of EMR on human heart tissue in 2D or 3D using the FDTD method. In addition, it is very important to study the thermal effect, power density, and SAR on the human heart layers by FDTD in further studies. A numerical simulation of EMR on other tissues of the human body should also be taken into consideration in the future. Also, it is recommended that a fast and effective numerical method be investigated for the 2D and MD human heart models and that an experimental method on SAR distribution be carried out to validate the outcomes from the simulation method.

Ethical considerations

Not applicable.

Conflict of Interest

The authors declare no conflicts of interest.

Funding

This research did not receive any financial support.

References

Aerts S, Deprez K, Verloock L, Olsen RG, Martens L, Tran P, Joseph W (2023) RF-EMF Exposure near 5G NR Small Cells. Sensors 23:3145. DOI: 10.3390/s23063145

Bai JZ, Ban Y, Bian JG, Chen AD, Chen HF, Chen HS, ..., Zhang C (2002) Measurements of the cross section for e+ e−→ hadrons at center-of-mass energies from 2 to 5 GeV. Physical Review Letters 88:101802. DOI: 10.1103/PhysRevLett.88.101802

Charny CK (1992) Mathematical models of bioheat transfer. Advances in heat transfer 22:19-155. DOI: 10.1016/S0065-2717(08)70344-7

Chua HT, Ng KC, Chakraborty A, Oo NM, Othman MA (2002) Adsorption characteristics of silica gel+ water systems. Journal of Chemical & Engineering Data 47:1177-1181. DOI: 10.1021/je0255067

El-dabe NT, Mohamed MA, El-Sayed AF (2003) Effects of microwave heating on the thermal states of biological tissues. African Journal of Biotechnology 2:453-459. DOI: 10.5897/AJB2003.000-1091

Elwasife K, Yasin G, Radwan E (2023) Estimation of electromagnetic radiation distribution in the human heart rate at different frequencies. Trends in Sciences 9 [accepted paper].

Elwasife KY (2019) Thermal effect of 1.8 GHz mobile phone radiation on dura tissue. Romanian Journal of Biophysics 29:51-58.

Elwasife KY (2012) Simulation of Thermal Global System Mobile Radiation in Retina Eye by FDTD Method. International Journal of Pure & Applied Sciences & Technology 10:44-50.

Giering K, Lamprecht I, Minet O, Handke A (1995) Determination of the specific heat capacity of healthy and tumorous human tissue. Thermochimica acta 251:199-205. DOI: 10.1016/0040-6031(94)02047-R

Goyal R, Bhargava R (2018) FEM simulation of EM field effect on body tissues with bio-nanofluid (blood with nanoparticles) for nanoparticle mediated hyperthermia. Mathematical biosciences 300:76-86. DOI: 10.1016/j.mbs.2018.03.016

Goyal R, Vafai K (2017) Electromagnetic field-induced thermal management of biological materials. Numerical Heat Transfer, Part A: Applications 72:275-290. DOI: 10.1080/10407782.2017.1372672

Haemmerich D (2022) Mathematical modeling of heat transfer in biological tissues (bioheat transfer). In Principles and Technologies for Electromagnetic Energy Based Therapies 1-24. DOI: 10.1016/B978-0-12-820594-5.00012-5

Hirata A, Laakso I, Oizumi T, Hanatani R, Chan KH, Wiart J (2013) The relationship between specific absorption rate and temperature elevation in anatomically based human body models for plane wave exposure from 30 MHz to 6 GHz. Physics in Medicine & Biology 58:903. DOI: 10.1088/0031-9155/58/4/903

Hristov AC, Tejasvi T, Wilcox RA (2019) Mycosis fungoides and Sézary syndrome: 2019 update on diagnosis, risk-stratification, and management. American journal of hematology 94:1027-1041. DOI: 10.1002/ajh.25577

Ismail N (2007) Modeling of electromagnetic wave penetration in a human head due to emissions from cellular phone (Doctoral dissertation, Universiti Tun Hussein Onn Malaysia). http://eprints.uthm.edu.my/2185/

Keangin P, Vafai K, Rattanadecho P (2013) Electromagnetic field effects on biological materials. International Journal of Heat and Mass Transfer 65:389-399. DOI: 10.1016/j.ijheatmasstransfer.2013.06.039

Khaled AR, Vafai K (2003) The role of porous media in modeling flow and heat transfer in biological tissues. International Journal of Heat and Mass Transfer 46:4989-5003. DOI: 10.1016/S0017-9310(03)00301-6

Liu DC, Ockerman HW (2001) Meat co-products. In Meat science and applications, pp 597-620, CRC Press.

Liu J (2001) Uncertainty Analysis for Temperature Prediction of Biological Bodies Subject to Randomly Spatial Heating. Journal of biomechanics 34:1637–1642. DOI: 10.1016/S0021-9290(01)00134-8

Mendibil U, Ruiz-Hernandez R, Retegi-Carrion S, Garcia-Urquia N, Olalde-Graells B, Abarrategi A (2020) Tissue-specific decellularization methods: rationale and strategies to achieve regenerative compounds. International journal of molecular sciences 21:5447. DOI: 10.3390/ijms21155447

Morimoto R, Laakso I, De Santis V, Hirata A (2016) Relationship between peak spatial-averaged specific absorption rate and peak temperature elevation in human head in frequency range of 1–30 GHz. Physics in Medicine & Biology 61:5406. DOI: 10.1088/0031-9155/61/14/5406

Petrofsky JS (2012) Resting blood flow in the skin: does it exist, and what is the influence of temperature, aging, and diabetes?. Journal of diabetes science and technology 6:674-685. DOI: 10.1177/193229681200600324

Ray LA, Heys JJ (2019) Fluid flow and mass transport in brain tissue. Fluids 4:196. DOI: 10.3390/fluids4040196

Romanenko S, Begley R, Harvey AR, Hool L, Wallace VP (2017) The interaction between electromagnetic fields at megahertz, gigahertz and terahertz frequencies with cells, tissues and organisms: risks and potential. Journal of The Royal Society Interface 14:20170585. DOI: 10.1098/rsif.2017.0585

Seetharaman R, Tharun M, Gayathri S, Mole SS, Anandan K (2022) Analysis of specific absorption rate and heat transfer in human head due to mobile phones. Materials Today: Proceedings 51:2365-2374. DOI: 10.1016/j.matpr.2021.11.582

Shbanah M, Kovács TA (2022) The Effects of Electromagnetic Waves on Human Health. In Security-Related Advanced Technologies in Critical Infrastructure Protection: Theoretical and Practical Approach, pp 161-167. Dordrecht: Springer Netherlands. DOI: 10.1007/978-94-024-2174-3_14

Susaki EA, Shimizu C, Kuno A, Tainaka K, Li X, Nishi K, ..., Ueda HR (2020) Versatile whole-organ/body staining and imaging based on electrolyte-gel properties of biological tissues. Nature communications 11:1982. DOI: 10.1038/s41467-020-15906-5

Vander Vorst A, Rosen A, Kotsuka Y (2006) RF/microwave interaction with biological tissues. John New Jersey: Wiley&Sons Inc.

Wang H, Burgei WA, Zhou H (2020) A concise model and analysis for heat-induced withdrawal reflex caused by millimeter wave radiation. American Journal of Operations Research 10:31-81. DOI: 10.4236/ajor.2020.102004

Weinbaum S, Jiji LM (1985) A new simplified bioheat equation for the effect of blood flow on local average tissue temperature. Journal of Biomechanical Engineering 107:131-139. DOI: 10.1115/1.3138533

Wessapan T, Rattanadecho P (2012) Specific absorption rate and temperature increase in human eye subjected to electromagnetic fields at 900 MHz. ASME Journal of Heat and Mass Transfer 134:091101. DOI: 10.1115/1.4006243

Wongchadakul P, Datta AK, Rattanadecho P (2023) Natural convection effects on heat transfer in a porous tissue in 3-D radiofrequency cardiac ablation. International Journal of Heat and Mass Transfer 204:123832. DOI: 10.1016/j.ijheatmasstransfer.2022.123832

Xu F, Lu TJ, Seffen KA, Ng EYK (2009) Mathematical modeling of skin bioheat transfer. Applied mechanics reviews 62:050801. DOI: 10.1115/1.3124646

Yamazaki Y, Danelishvili L, Wu M, Hidaka E, Katsuyama T, Stang B, ... Bermudez LE (2006) The ability to form biofilm influences Mycobacterium avium invasion and translocation of bronchial epithelial cells. Cellular microbiology 8:806-814. DOI: 10.1111/j.1462-5822.2005.00667.x

Yi M, Chi Y, Wu B, Zhao Y, Su T, Qi Y (2023) Safety assessment of electromagnetic radiation from mobile phone antennas to the human head. International Journal of Energy 2:23-26. DOI: 10.54097/ije.v2i2.7320

Zhu L, Bischof J (2019) A New Simplified Bioheat Equation for the Effect of Blood Flow on Local Average Tissue Temperature. Journal of Biomechanical Engineering 107:131-139. DOI: 10.1115/1.3138533

Zhu L, Diao C (2001) Theoretical simulation of temperature distribution in the brain during mild hypothermia treatment for brain injury. Medical and Biological Engineering and Computing 39:681-687. DOI: 10.1007/BF02345442